Electronic Supplementary Material (ESI) for Catalysis Science & Technology.
This journal is © The Royal Society of Chemistry 2021

Syngas to light olefins over La doped $Zn_xAl_yO_z$ composite and SAPO-34 hybrid catalysts

G. Raveendra, ‡ Baorun Ma, ‡ Xiaohui Liu*, Yong Guo and Yanqin Wang*

Shanghai Key Laboratory of Functional Materials Chemistry and Research Institute of Industrial Catalysis, School of Chemistry and Molecular Engineering, East China University of Science and Technology, Meilong Road 130, Shanghai 200237, China

Table S1. Composition and textural properties of $La/Zn_xAl_yO_z$ prepared with different precipitating agents at pH 7.

Catalysts	ICP-OES Weight ratio of La/Zn/Al	BET Surface area (m^2/g)[a]	Pore volume (cm^3/g)[b]	Pore diameter (nm)[c]
Parent $ZnO-Al_2O_3(NH_4OH)$	-	91	0.06	2.71
$La/Zn_xAl_yO_z$-AH-7	0.33/20/42	196	0.10	2.51
$La/Zn_xAl_yO_z$-AC-7	0.34/19/40	198	0.10	2.62
$La/Zn_xAl_yO_z$-SC-7	0.37/19/41	182	0.12	2.69
$La/Zn_xAl_yO_z$-SH-7	0.32/20/43	88	0.06	3.44

[a] Calculated by the BET equation. [b] BJH desorption average pore volume. [c] BJH desorption pore diameter.

Table S2. Composition and textural properties of $La/Zn_xAl_yO_z$ prepared with NH_4OH as precipitate agent at different pH.

Catalysts	ICP-OES Weight ratio of La/Zn/Al	BET Surface area (m^2/g)[a]	Pore volume (cm^3/g)[b]	Pore diameter (nm)[c]
$La/Zn_xAl_yO_z$-AH-6	0.30/19/42	212	0.14	3.07
$La/Zn_xAl_yO_z$-AH-7	0.37/19/42	196	0.10	2.51
$La/Zn_xAl_yO_z$-AH-8	0.34/19/42	170	0.09	2.22
$La/Zn_xAl_yO_z$-AH-9	0.35/19/40	159	0.09	2.36
$La/Zn_xAl_yO_z$-AH-7 /SAPO-34 Fresh	-	205	0.124	2.42
$La/Zn_xAl_yO_z$-AH-7 /SAPO-34 used	-	156	0.12	3.24

[a] Calculated by the BET equation. [b] BJH desorption average pore volume. [c] BJH desorption pore diameter

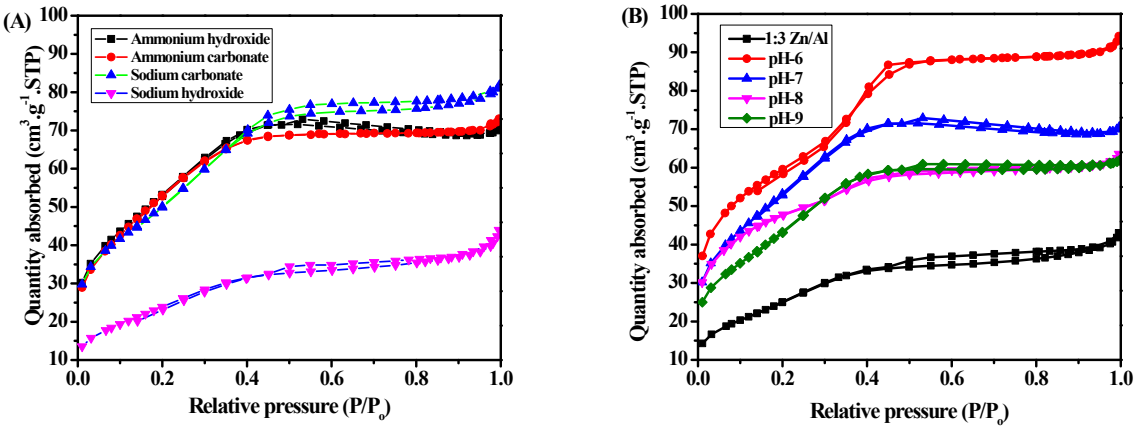

Fig. S1 N_2-adsorption-desorption isotherms of (A) La doped $Zn_xAl_yO_z$ prepared with different precipitating agents at pH=7. (B) Parent and La doped $Zn_xAl_yO_z$ prepared at different pH values using NH_4OH as the precipitating agent.

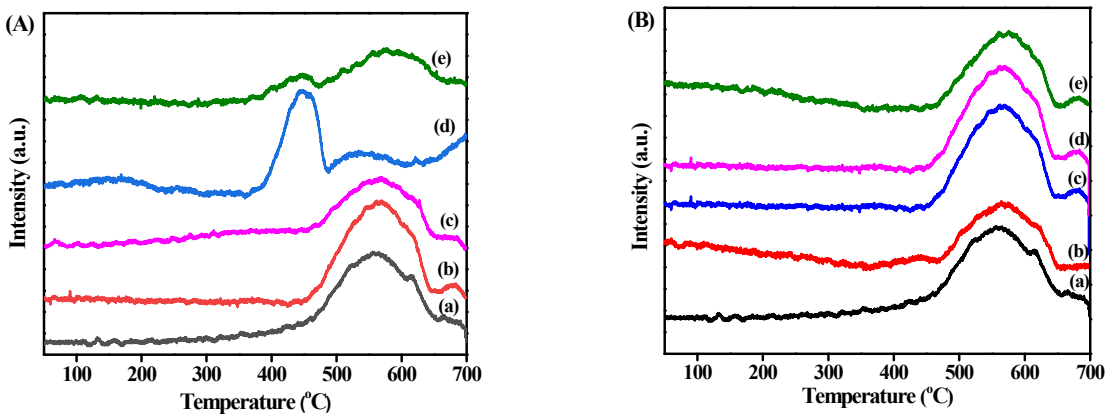

Fig. S2. H_2-TPR profiles of various samples. **(A)** Parent and with different precipitating agents at pH=7: (a) Parent; (b) La/$Zn_xAl_yO_z$-AH; (c) La/$Zn_xAl_yO_z$-AC; (d) La/$Zn_xAl_yO_z$-SC and (e) La/$Zn_xAl_yO_z$-SH. **(B)** At different pH values using NH_4OH as the precipitating agent, (a) Parent; (b) 6; (c) 7; (d) 8 and (e) 9.

H_2-temperature-programmed reduction (H_2-TPR) profiles were measured by Huasi DAS-7200 automatic chemisorption instrument. Before each measurement, to remove the physically adsorbed species on the surface of the catalyst, the samples were pretreated by using pure Ar at 150 °C for 30 min and then cooled to room temperature. A reducing gas containing 5%H_2/95%Ar was employed at a flow rate of 30 ml·min^{-1} and a heating rate of 10 °C·min^{-1} from ambient temperature to 600 °C, using a TCD detector to monitor the H_2 consumption.

1. Activity results

1.1 Effect of reaction temperature

The effect of reaction temperature on syngas to light olefins synthesis over La/$Zn_xAl_yO_z$–SAPO-34 hybrid catalyst is shown in Fig. S3 (A). At lower reaction temperature of 370 ^{o}C, the catalyst exhibited 10.3% of CO conversion and light olefins selectivity was 83.0%. With increase of reaction temperature from 370 °C to 380 °C, the conversion of CO increased from 10.3% to 14.1% and light olefins selectivity is slightly decreased from 83% to 81.1%.Upon increasing the reaction temperature to 400 ^{o} C, the conversion of CO increased to 16.7%, but the selectivity of light olefins decreased to 68.0%, with the increase of paraffins selectivity. That means higher temperature favors methane formation and the hydrogenation of olefins to paraffins. Based on these results, 380 °C reaction temperature is considered as the best temperature for better CO conversion and light olefins selectivity.

1.2 Reaction pressure

The effect of reaction pressure on La/$Zn_xAl_yO_z$–SAPO-34 hybrid catalysts tested for syngas to light olefins synthesis and the results are shown in Fig. S3 (B). At lower reaction pressure of 1.0 MPa, the CO conversion is 8.6% and light olefins selectivity is 79.7%, with methane selectivity

of 7.3% and paraffins selectivity of 12.9%. When the reaction pressure was increased from 1 MPa to 2 MPa, the conversion of CO was increased to 14.1% and light olefins selectivity was slightly increased to 81.1%, with methane selectivity of 4.3% and paraffins selectivity of 14.6%. When further increase the reaction pressure from 2 MPa to 3 MPa, the conversion of CO was decreased to 13.0% and light olefins selectivity was also decreased to 74.0%. This is may be due to a high occupation of the surface with H_2, which may inhibit adsorption and reaction of CO over the catalyst surface [1]. Therefore, based on the results, it can be stated that the catalyst shows a good catalytic performance at moderate reaction pressure of 2 MPa.

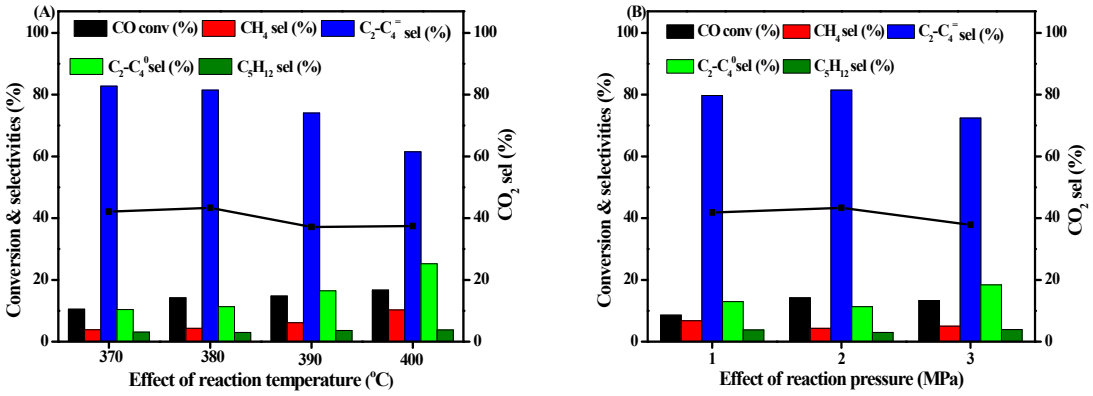

Fig. S3. (A) Effect of reaction temperature over La/$Zn_xAl_yO_z$-AH-7-SAPO-34 hybrid catalysts; (B) Effect of reaction pressure over La/$Zn_xAl_yO_z$-AH-7-SAPO-34 hybrid catalysts.

Reaction conditions: catalyst 0.50 g; H_2/CO=2:1; 2 MPa; 30 ml·min^{-1}; time on stream 8 h; S2 (A) 370-400 °C and S2; (B) 1–3 MPa, 380 °C. Selectivity was calculated on a molar carbon basis for CO hydrogenation; the formation of CO_2 by the WGS reaction. The selectivities of the products are CO_2 free.

1.3 Gas hourly space velocity (GHSV)

Fig. S4 (A) shows the effect of GHSV on catalytic performance of La/$Zn_xAl_yO_z$–SAPO-34 hybrid catalyst for syngas to light olefins synthesis. The effect of GHSV was evaluated at 3000, 3600, and 4200 $ml.g^{-1}.h^{-1}$. At lower GHSV of 3000 $ml.g^{-1}.h^{-1}$, the conversion of CO is 14.6% and light olefins selectivity is 76.0%, with methane selectivity of 5.4% and paraffins selectivity of 18.6%. When increase the GHSV flow rate, the conversion of CO was decreased to 14.1%, but the light olefins selectivity is slightly increased to 81.1%. Further increase of GHSV to 4200$ml.g^{-1}.h^{-1}$, the conversion of CO was decreased to 11.3% and light olefins selectivity slightly decreased to 79.0%. From the above results suggested that the higher CO conversion obtained at lower GHSV of 3000 $ml.g^{-1}.h^{-1}$ which is may be due to a longer contact time of CO molecules with hybrid catalysts, thus enhanced the catalytic activity. But lower GHSV leads to the hydrogenation of light olefins to paraffins. With increase of GHSV rate, the CO conversion was decreased, this is mainly due to the retention time of CO stayed on the hybrid catalyst surface is too short to reaction. Among these results, the GHSV of 3600 $ml.g^{-1}.h^{-1}$ is better for the CO conversion and high selectivity to light olefins.

1.4 Effect of Si/Al ratio of SAPO-34 zeolite

The acidic property of SAPO-34 zeolite also plays a vital role for the catalytic performance of the hybrid catalysts. The effects of different Si/Al ratios were studied and obtained results are shown in Fig. S4 (B). The lower silica content of SAPO-34(0.1) catalyst exhibits 8.6% CO conversion and 80.5% selectivity to $C_2^=$–$C_4^=$. Whereas, with increasing the Si/Al from 0.1 to 0.15, the conversion of CO is 11.5% and the selectivity to $C_2^=$–$C_4^=$ is varied 83.4 %. Further increasing the Si/Al ratio from 0.15 to 0.2 in SAPO-34, the conversion of CO is increased to 14.1%, but the $C_2^=$–$C_4^=$ selectivity is slightly decreased to 81.0%. Thus, higher Si content in SAPO-34 (0.2) sample showed higher activity. The Si incorporation into the AlPO framework in SAPO-34 is a

key factor for acid site generation [2]. All of the SAPO-34 samples with different Si/Al ratio, the number of acid sites increased with increase of Si content for SAPO-34(0.2), as shown in Table S3. The conversion of CO to light olefins synthesis should depend on the amount of acid sites of zeolite catalysts. Therefore, SAPO-34 (0.2) with the higher acidity was advantageous for the higher activity.

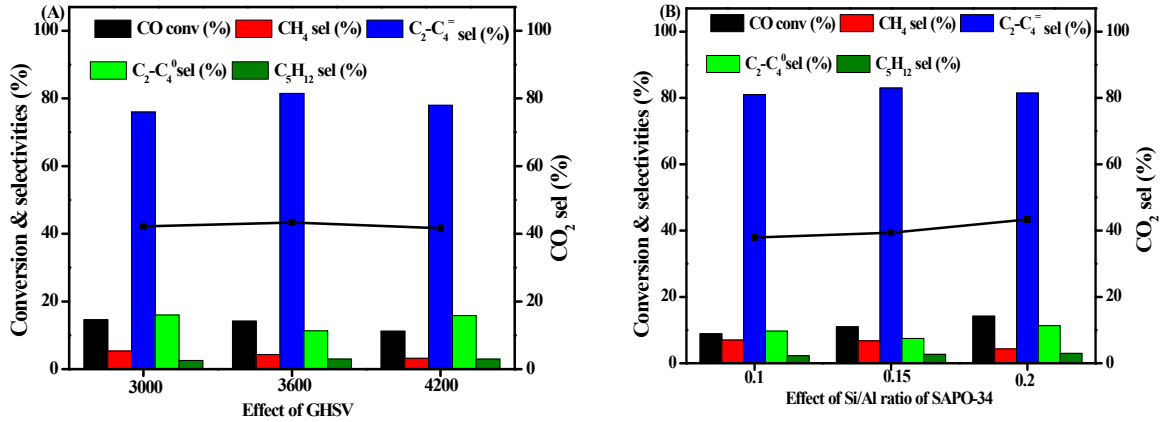

Fig. S4 (A) Effect of GHSV over La/$Zn_xAl_yO_z$–AH-7-SAPO-34 hybrid catalysts (B) Effect of Si/Al ratio of SAPO-34

Reaction conditions: catalyst 0.50 g; H_2/CO=2:1; 2 MPa; 30 ml·min^{-1}; time on stream 8 h; 380 ^{o}C. Selectivity was calculated on a molar carbon basis for CO hydrogenation; the formation of CO_2 by the WGS reaction. The selectivities of the products are CO_2 free.

Table S3. Textural properties of SAPO-34 zeolites

Catalysts	BET Surface area (m^2/g)[a]	External surface area(m^2/g)	Pore volume(cm^3/g)[b]	Pore diameter(nm)[c]	Acidity (mmol/g)[d]
SAPO-34 (0.1)	652	24	0.30	1.85	0.98

SAPO-34 (0.15)	551	23	0.26	1.95	1.31
SAPO-34 (0.2)	637	15	0.29	1.87	1.02

[a] Calculated by the BET equation, [b] BJH desorption average pore volume, [c] BJH desorption pore diameter, [d] Acidity values from NH_3-TPD.

1.5 Coke formation

To measure the amount of coke deposited on the spent catalyst, TGA was performed, and the TGA curves of the catalysts are shown in Fig. S5. From the previous reports, the fresh hybrid catalyst the weight loss from 30 to 110 °C due to the removal of physically adsorbed water and part of crystal water from $Al_2O_3 \cdot 3H_2O$ [3]. The weight loss from 110 to 220 °C due to the phase transition from $Al_2O_3 \cdot H_2O$ to AlOOH [4]. For the hybrid catalyst of La doped ZnxAlyOz with SAPO-34 hybrid catalyst, during the reaction, some amount of water formed on the catalyst surface, which it is clearly seen at lower temperature. This is mainly due to the coke formation on the catalyst surface for the weight loss at higher temperature from 250–580 °C [5].

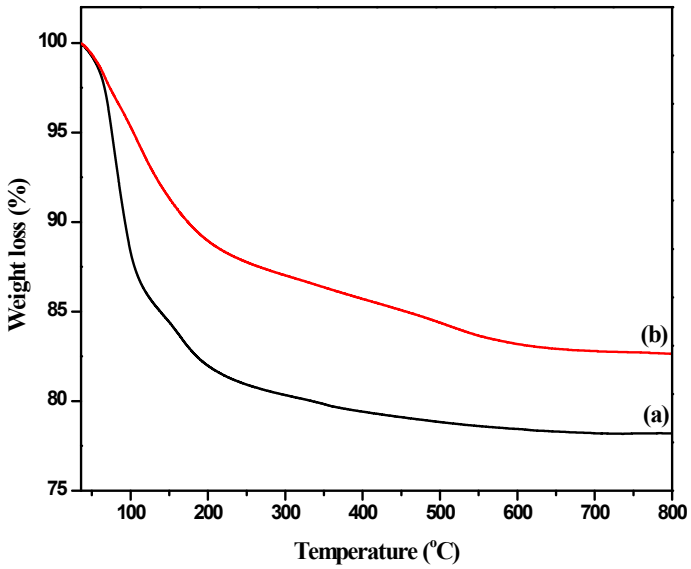

Fig. S5 TGA analysis of (a) Fresh (b) Used La/$Zn_xAl_yO_z$-SAPO-34 hybrid catalyst.

2. Characterizations

XRD patterns of different Si/Al ratio of SAPO-34 zeolite samples are shown in Fig. S6. The main characteristic diffraction peaks of 2θ values at 9.6°, 13°, 15.9°, 17.7°, 20.7°, 24.9°, 26° and 31° which are mainly attributed to the chabazite structure (CHA) of SAPO-34 zeolite [6]. All of the SAPO-34 samples exhibit the characteristic peaks which are in good agreement with those patterns of SAPO-34 zeolite. The lower Si content of SAPO-34 (0.1) sample shows lower 2θ values, while with increase of silica content in SAPO-34 (0.15) and SAPO-34 (0.2) zeolite the peaks slightly shifted towards higher 2θ values as a result of change in framework composition due to the expansion/contraction of the unit cell.

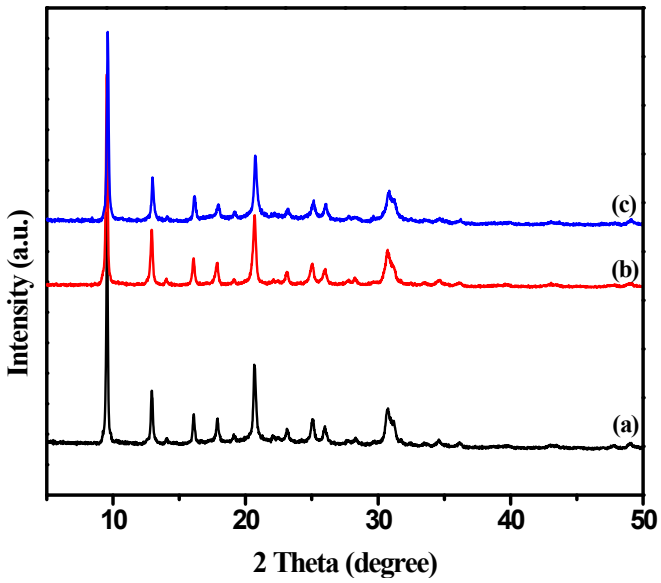

Fig. S6 XRD patterns of different Si/Al ratio of SAPO-34 zeolites (a) 0.1 (b) 0.15 (c) 0.2

The textural properties of different Si/Al ratios of SAPO-34 zeolite are presented in Table S3. The BET surface area of SAPO-34 with Si/Al ratio of 0.1, 0.15 and 0.2 (0.1) are 651, 551 and 641 $m^2 g^{-1}$, respectively. It could be seen that all of these samples also exhibited external surface

area, which was mainly due to some defects on the external surface as well as the inter crystalline porosity.

NH_3-TPD technique was used to characterize the acidic properties of SAPO-34 zeolites with different Si/Al ratios and La/$Zn_xAl_yO_z$-SAPO-34 hybrid catalyst are shown in Fig. S7 and Fig. S8. All the samples show two desorption peaks at 100–200 °C and 300–400 °C. The low-temperature desorption peak corresponds to the ammonia adsorbed on lattice defective structural OH groups (Si(OH) P-OH and Al-OH) [7]. In addition, the high temperature desorption peak is related to the ammonia attached to Brönsted acid sites in the form of bridging hydroxyl groups of Si(OH)Al [8]. The strong acid sites are the primary active sites for MTO reactions [9].

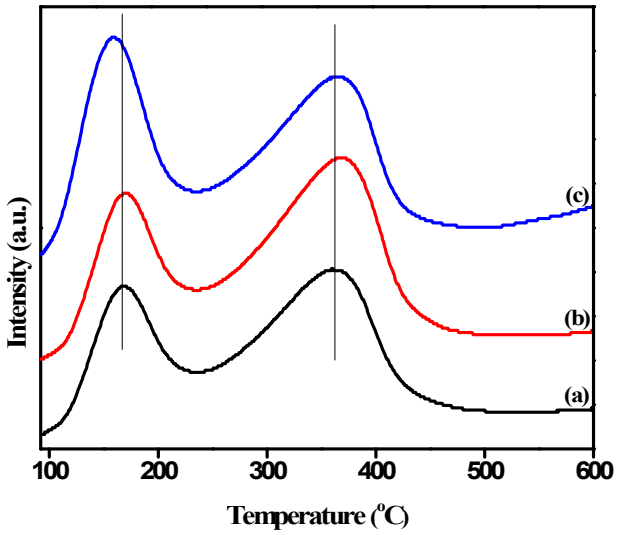

Fig. S7 NH_3-TPD profiles of different Si/Al ratio of SAPO-34 zeolites (a) 0.1 (b) 0.15 (c) 0.2

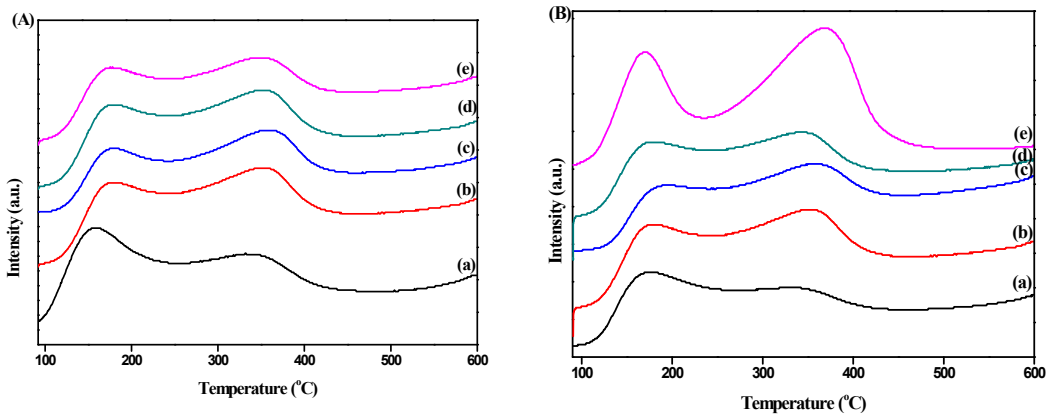

Fig. S8 NH_3-TPD profiles of La/$Zn_xAl_yO_z$-SAPO-34 hybrid catalyst. (A) Using different precipitating agents (a) Ammonium hydroxide; (b) Ammonium carbonate; (c) Sodium carbonate and (d) Sodium hydroxide. (B) At different pH values (a) 6; (b) 7; (c) 8; (d) 9 and (e) only SAPO-34.

References

[1] O. A. Ojelade, S. F. Zaman, M. A. Daous, A. A .Al-Zahrani, AliS. Malik, H. Driss, Genrikh Shterk, J. Gascon, Applied Catalysis A: General, 2019, 584, 117185.

[2] M. Ghavipour, A. S. Mehr, Y.Wang, R. M. Behbahani, S. Hajimirzaee and K. Bahrami, RSC Adv., 2016, 6, 17583–17594.

[3] M. Mokhtar, A. Inayat, J. Ofili and W. Schwieger, Appl. Clay Sci., 2010, 50, 17668.

[4] A. A. Da silva, A. Goncalves, M.R. Davolos, J. Sol. gel Sci. Tech. 2009, 49, 101.

[5] Y. Huang, H. Ma, Z. Xu, W. Qian, H. Zhang, W. Ying, Fuel, **2020,** 273, 117771.

[6] G. Chen, Q. Sun and J. Yu, Chem. Commun., 2017, 53, 13328–13331.

[7] H. Akhoundzadeh, M. Taghizadeh, H.SharifiPajaie, Particuology, 2018, 40, 113–122.

[8] J. Chen, J. Li, C.Yuan, S. Xu, Y.Wei, Q.Wang,Y.Zhou, J. Wang, M. Zhang,Y.He, S. Xua and Z. Liu, Catal. Sci. Technol., 2014, 4, 3268–3277.

[9] C.Y. Kong, J. Zhu, S.Y. Liu, Y. Wang, RSC Adv., 2017, 7, 39889–39898.